Ground-state blockade of Rydberg atoms and application in entanglement generation

X. Q. Shao,* D. X. Li, Y. Q. Ji, J. H. Wu, and X. X. Yi

Center for Quantum Sciences and School of Physics, Northeast Normal University, Changchun 130024, People's Republic of China and Center for Advanced Optoelectronic Functional Materials Research, and Key Laboratory for UV Light-Emitting Materials and Technology of Ministry of Education, Northeast Normal University, Changchun 130024, China

(Received 24 April 2017; published 24 July 2017)

We propose a mechanism of ground-state blockade between two N-type Rydberg atoms by virtue of the Rydberg-antiblockade effect and the Raman transition. Inspired by the quantum Zeno effect, the strong Rydberg antiblockade interaction plays a role in frequently measuring one ground state of two, leading to a blockade effect for double occupation of the corresponding quantum state. By encoding the logic qubits into the ground states, we efficiently avoid the spontaneous emission of the excited Rydberg state and maintain the nonlinear Rydberg-Rydberg interaction at the same time. As applications, we discuss in detail the feasibility of preparing two-atom and three-atom entanglement with ground-state blockade in closed and open systems, respectively, which shows that a high fidelity of the entangled state can be obtained with current experimental parameters.

DOI: 10.1103/PhysRevA.96.012328

I. INTRODUCTION

Neutral atoms are considered a good candidate for quantum information processing. Their stable atomic hyperfine energy states, especially suited for encoding logic qubits, are easily controllable and measurable by making use of a resonant laser pulse. On the other hand, they possess state-dependent interaction properties. When an atom is excited to the high-lying Rydberg states, the powerful dipole-dipole interaction or van der Waals interaction will significantly shift its surrounding atomic energy levels of Rydberg states, thereby inhibiting the double or more excitations of Rydberg states, and this is the so-called Rydberg blockade phenomenon. This effect can make the atomic ensemble effectively behave as a single two-level system; thus the idea of Jaksch *et al.* [1] for using dipolar Rydberg interactions to implement a two-qubit universal quantum gate was quickly extended to a mesoscopic regime of many-atom ensemble qubits by Lukin *et al.* [2]. In 2009, the mechanism of Rydberg blockade was verified in experiment and two groups independently claimed that a single Rydberg-excited rubidium atom blocks excitation of a second atom set about 4 and 10 μm apart [3,4], respectively. Recently, the Rydberg blockade has been used extensively in various subfields of quantum information processing, such as quantum entanglement [5–8], quantum algorithms [9–11], quantum simulators [12,13], single-photon switch [14], quantum repeaters [15–17], etc.

In contrast to the Rydberg blockade, as the shifting energy of Rydberg states is compensated by the two-photon detuning, the effect of the Rydberg antiblockade occurs, which favors a resonant two-photon transition, but counters a single-photon transition. The antiblockade in Rydberg excitation was initially predicted by Ates *et al.* in the two-step excitation scheme of creating an ultracold Rydberg gas [18] and then observed experimentally by Amthor *et al.* using a time-resolved spectroscopic measurement of the Penning ionization signal [19]. With regard to quantum information processing, the Rydberg antiblockade provides researchers with brand new ideas. Combined with asymmetric Rydberg couplings and dissipative dynamics, the Rydberg antiblockade has been exploited to generate high-fidelity two-qubit Bell states and three-dimensional entanglement [20,21]. It has also been instrumental in fast synthesis of multiqubit logic gates [22,23].

We note that a resonant excitation of the Rydberg state is necessary for realizing most Rydberg-blockade-based schemes. This requirement may cause decoherence to the system of interest due to the spontaneous emission of the excited Rydberg state, although it is considered that the Rydberg state with a large principle quantum number has a small decay rate [24]. If the excited-state blockade of Rydberg atoms is replaced with a ground-state blockade, we are able to minimize the effect of atomic decay and further improve the quality of quantum information processing with Rydberg atoms. Nevertheless, the interaction of natural ground-state neutral atoms is less than 1 Hz at spacings greater than 1 μm [25], which is unsuitable for fulfilling the blockade condition.

In this work, we put forward an efficient scheme for blocking ground states of Rydberg atoms. Our idea comes from the quantum Zeno effect [26,27], i.e., one can freeze the evolution of a quantum system by measuring it frequently enough in its known initial state, and the same conclusion can also be made by making use of a strong continuous coupling without resorting to von Neumann's projections [28]. For the current scheme, the dynamical evolution of the system is governed by a weak Raman coupling with strength $\Omega_{\rm eff}$. A relatively strong Rydberg antiblockade interaction with strength λ, acting as a measuring device, is used to observe the evolution of the double occupation of a certain ground state. In the limit $\lambda/\Omega_{\rm eff} \gg 1$, the ground-state blockade for Rydberg atoms is achieved. As its application, we discuss in detail the prominent advantage of ground-state blockade in terms of preparing entanglement via a shortcut to adiabatic passage and quantum-jump-based feedback control, respectively.

The remainder of the paper is organized as follows. We first establish the theoretical model of the ground-state blockade mechanism in Sec. II. Then we investigate the robustness for preparation of the maximally entangled state based on the ground-state Rybderg blockade in a closed system and in an open system, respectively, in Secs. III and IV. Then we

*Corresponding author: shaoxq644@nenu.edu.cn

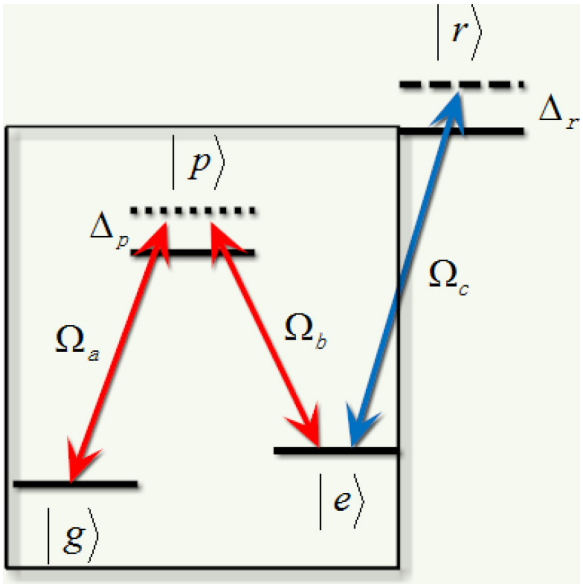

FIG. 1. Schematic view of the atomic-level configuration. The ground states $|g\rangle$ and $|e\rangle$ are dispersively coupled to the excited state $|p\rangle$ with Rabi frequencies Ω_a and Ω_b, respectively. An additional classical field drives the transition $|e\rangle \leftrightarrow |r\rangle$ with the Rabi frequency Ω_c. $\Delta_{p(r)}$ represents the corresponding single-photon detuning parameter.

directly generalize the above schemes to the case of three-atom entanglement in Sec. V. Finally, we give a summary of our proposal in Sec. VI.

II. GROUND-STATE BLOCKADE MECHANISM BETWEEN TWO ATOMS

We consider a system consisting of two N-type four-level Rydberg atoms, and the relevant configuration of the atomic level is illustrated in Fig. 1. The ground states $|g\rangle$ and $|e\rangle$ are dispersively coupled to the excited state $|p\rangle$ by two classical fields with Rabi frequencies Ω_a and Ω_b and a common detuning $-\Delta_p$. And the ground state $|e\rangle$ can be pumped into the excited Rydberg state $|r\rangle$ by a driving field with Rabi frequency Ω_c, detuned by $-\Delta_r$. In the interaction picture with respect to a rotating frame, the Hamiltonian of the system reads ($\hbar = 1$)

$$H_I = \sum_{i=1}^{2} \Omega_a |p\rangle_i\langle g| + \Omega_b |p\rangle_i\langle e| + \Omega_c |r\rangle_i\langle e| + \text{H.c.} - \sum_{i=1}^{2} \Delta_p |p\rangle_i\langle p| + (U - 2\Delta_r)|rr\rangle\langle rr|, \quad (1)$$

where U represents the Rydberg-mediated interaction as two atoms simultaneously occupy the Rydberg state. This kind of nonlinear interaction originates from the dipole-dipole potential with energy C_3/r^3 or the long-range van der Waals interaction C_6/r^6, with r being the distance between two Rydberg atoms and $C_{3(6)}$ depending on the quantum numbers of the Rydberg state [29,30]. Through the standard second-order perturbation theory, we may adiabatically eliminate the excited state $|p\rangle$ and the single-atom Rydberg state $|r\rangle$ in the regime of the large detuning limits $\Delta_p \gg \{\Omega_a, \Omega_b\}$ and $\Delta_r \gg \Omega_c$. Then we obtain an effective Hamiltonian as

$$H_{\text{eff}} = \sum_{i=1}^{2} \frac{\Omega_a^2}{\Delta_p} |g\rangle_i\langle g| + \left(\frac{\Omega_b^2}{\Delta_p} + \frac{\Omega_c^2}{\Delta_r}\right)|e\rangle_i\langle e| + \left[\frac{2\Omega_c^2}{\Delta_r}|ee\rangle\langle rr| + \sum_{i=1}^{2} \frac{\Omega_a\Omega_b}{\Delta_p}|g\rangle_i\langle e| + \text{H.c.}\right] + \left(U - 2\Delta_r + \frac{2\Omega_c^2}{\Delta_r}\right)|rr\rangle\langle rr|. \quad (2)$$

The first two terms cause unwanted shifts to our system, which need to be canceled via introducing other ancillary levels. The Stark shift in the last term $2\Omega_c^2/\Delta_r$ stems from the two-photon transition $|ee\rangle \leftrightarrow \langle rr|$. Now the above Hamiltonian can be rewritten in a concise form:

$$H_{\text{eff}} = \sum_{i=1}^{2} \Omega_{\text{eff}} |g\rangle_i\langle e| + \lambda |ee\rangle\langle rr| + \text{H.c.} + \Delta |rr\rangle\langle rr|, \quad (3)$$

where $\Omega_{\text{eff}} = \Omega_a\Omega_b/\Delta_p$, $\lambda = 2\Omega_c^2/\Delta_r$, and $\Delta = U - 2\Delta_r + 2\Omega_c^2/\Delta_r$. We now divide Eq. (3) into two parts, i.e., $H_{\text{eff}} = H_\alpha + H_\beta$, where $H_\alpha = \sum_{i=1}^{2} \Omega_{\text{eff}}(|g\rangle_i\langle e| + |e\rangle_i\langle g|)$ describes the Raman transition of two ground states, and $H_\beta = \lambda(|ee\rangle\langle rr| + |rr\rangle\langle ee|) + \Delta|rr\rangle\langle rr|$, which represents the Rydberg antiblockade interaction. The Hamiltonian H_β can be diagonalized by the eigenstates $|\Psi_+\rangle = \cos\alpha|rr\rangle + \sin\alpha|ee\rangle$ and $|\Psi_-\rangle = \sin\alpha|rr\rangle - \cos\alpha|ee\rangle$, corresponding to eigenvalues $E_+ = (\Delta + \sqrt{\Delta^2 + 4\lambda^2})/2$ and

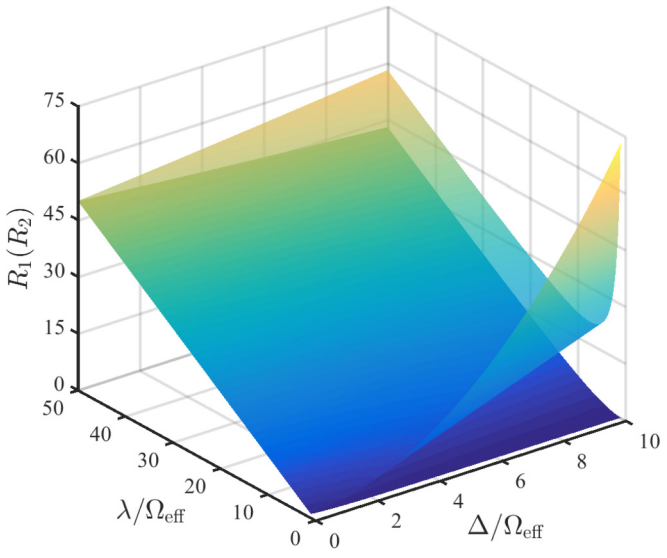

FIG. 2. The ratios R_1 (upper surface) and R_2 (lower surface) are plotted as functions $\Delta/\Omega_{\text{eff}}$ and $\lambda/\Omega_{\text{eff}}$, where $R_1 = |E_+/(\sqrt{2}\Omega_{\text{eff}}\sin\alpha)|$ and $R_2 = |E_-/(\sqrt{2}\Omega_{\text{eff}}\cos\alpha)|$.

TABLE I. Maximal populations of relevant quantum states corresponding to three specific ratios of R_1 (R_2) at $\Delta = 0$.

R_1	R_2	$\|gg\rangle$	$\|T\rangle$	$\|ee\rangle$
10	10	1.00	0.9673	0.0015
20	20	1.00	0.9916	1.0121×10^{-4}
50	50	1.00	0.9963	2.7228×10^{-6}

$E_- = (\Delta - \sqrt{\Delta^2 + 4\lambda^2})/2$, respectively, and $\alpha = \arctan[2\lambda/(\Delta + \sqrt{\Delta^2 + 4\lambda^2})]$. Thus we have

$$H_{\rm eff} = \sqrt{2}\Omega_{\rm eff}|gg\rangle\frac{1}{\sqrt{2}}(\langle ge| + \langle eg|) + \sqrt{2}\Omega_{\rm eff}(\sin\alpha|\Psi_+\rangle - \cos\alpha|\Psi_-\rangle)\frac{1}{\sqrt{2}}(\langle ge| + \langle eg|) + \text{H.c.} + E_+|\Psi_+\rangle\langle\Psi_+| + E_-|\Psi_-\rangle\langle\Psi_-|. \quad (4)$$

It is shown that the ground state $|gg\rangle$ resonantly interacts with the entangled state $(|ge\rangle + |eg\rangle)/\sqrt{2}$ with coupling constant $\sqrt{2}\Omega_{\rm eff}$, and $(|ge\rangle + |eg\rangle)/\sqrt{2}$ is then coupled to the state $|\Psi_+\rangle$ ($|\Psi_-\rangle$) with strength $\sqrt{2}\Omega_{\rm eff}\sin\alpha$ ($\sqrt{2}\Omega_{\rm eff}\cos\alpha$), detuning E_+ (E_-). In the limits of $R_1 = |E_+/(\sqrt{2}\Omega_{\rm eff}\sin\alpha)| \gg 1$ and $R_2 = |E_-/(\sqrt{2}\Omega_{\rm eff}\cos\alpha)| \gg 1$, the high-frequency oscillating terms may be neglected and an approximated ground-state blockade Hamiltonian is obtained:

$$H_{gb} = \sqrt{2}\Omega_{\rm eff}|gg\rangle\frac{1}{\sqrt{2}}(\langle ge| + \langle eg|) + \text{H.c.}. \quad (5)$$

In Fig. 2, the ratio R_1 (R_2) is plotted as a function of $\Delta/\Omega_{\rm eff}$ and $\lambda/\Omega_{\rm eff}$, which is explicit to determine the values of λ and Δ so as to get a better ground-state blockade effect. For instance, Table I lists the maximal populations of states $|T\rangle = (|ge\rangle + |eg\rangle)/\sqrt{2}$ and $|ee\rangle$ from the initial state $|gg\rangle$. The corresponding results are extracted from the numerical simulation of Eq. (1), which signifies that R_1 (R_2) $= 20$ is big enough for the occurrence of ground-state blockade. In the following, we reveal the advantage of ground-state blockade in the preparation of quantum entanglement by setting $\Delta = 0$ for simplicity.

III. ROBUST ENTANGLEMENT VIA SHORTCUT TO ADIABATIC PASSAGE

Before preparation of the entangled state, let us first discuss the robustness of quantum state transfer for a single Λ-type atom, in the presence of spontaneous emission. It has a guiding significance on the choice of parameters for the experimental realization of entanglement. The studied system is shown in the box in Fig. 1; the atom can spontaneously decay with the same rate $\gamma_p/2$ from the excited state $|p\rangle$ into the ground states $|g\rangle$ and $|e\rangle$, respectively. Hence the complete master equation describing the dynamics of this system reads

$$\dot{\rho}_{sgl} = -i[H_{sgl}, \rho_{sgl}] + \frac{\gamma_p}{2}\sum_{m=g,e}\mathcal{D}[\sigma_-^m]\rho_{sgl}, \quad (6)$$

where $H_{sgl} = \Omega_a|p\rangle\langle g| + \Omega_b|p\rangle\langle e| + \text{H.c.} - \Delta_p|p\rangle\langle p|$ and $\mathcal{D}[\sigma_-^m]\rho_{sgl} = \sigma_-^m\rho_{sgl}\sigma_+^m - \{\sigma_+^m\sigma_-^m, \rho_{sgl}\}/2$. $\sigma_-^m = (\sigma_+^m)^\dagger$ is the lowering operator of the atom from the excited state $|p\rangle$ to the ground state $|m\rangle$. After adiabatically eliminating the excited state $|p\rangle$ under the large detuning condition $\Delta_p \gg \{\Omega_a, \Omega_b\}$, the single-atom master equation is reduced to

$$\dot{\rho}_{sgl} = -i[H_{rd}, \rho_{sgl}] + \sum_{m=g,e}\mathcal{D}[R_{mp}]\rho_{sgl}, \quad (7)$$

where H_{rd} denotes the effective Hamiltonian of Raman transition between states $|g\rangle$ and $|e\rangle$ with coupling strength $\Omega_{\rm eff}$ and

$$R_{mp} = \sqrt{\frac{\gamma_p}{2}}|m\rangle\left(\frac{\Omega_a}{\Delta_p}\langle g| + \frac{\Omega_b}{\Delta_p}\langle e|\right), (m = g, e), \quad (8)$$

represents the effective decay operator [31–33]. Equation (8) gives a quantitative relationship among the Rabi frequency of classical fields, the frequency detuning parameter, and the spontaneous emission rate of the atom. It can be directly seen that the decaying rate is reduced to

$$\gamma_{\rm eff} = \frac{\gamma_p}{2}\frac{\Omega^2}{\Delta_p^2} = \frac{\gamma_p}{2\Delta_p}\Omega_{\rm eff}, \quad (9)$$

where we have assumed $\Omega = \Omega_{a(b)}$ for the sake of convenience. Therefore, we may reduce the effect of spontaneous emission by enlarging the value of the detuning Δ_p for implementing the quantum state transfer, even without changing the interaction time of the system. Figure 3 characterizes the population $P_e(t) = \langle e|\rho_{sgl}(t)|e\rangle$ of the state $|e\rangle$ in the process of quantum state transfer from the initial state $|g\rangle$ corresponding to different detuning and decoherence parameters. The effective Raman coupling strength is fixed at $\Omega_{\rm eff} = 0.004\Omega_c$. For $\Delta_p = 20\Omega_c$, the maximal state transfer efficiency is 96.21% as $\gamma_p = \Omega_c$ (dotted line), and this value is promoted to 99.51% for $\Delta_p = 160\Omega_c$ (dash-dotted line), which is very close to the ideal case 99.96% (solid line). Hence one can see that a large

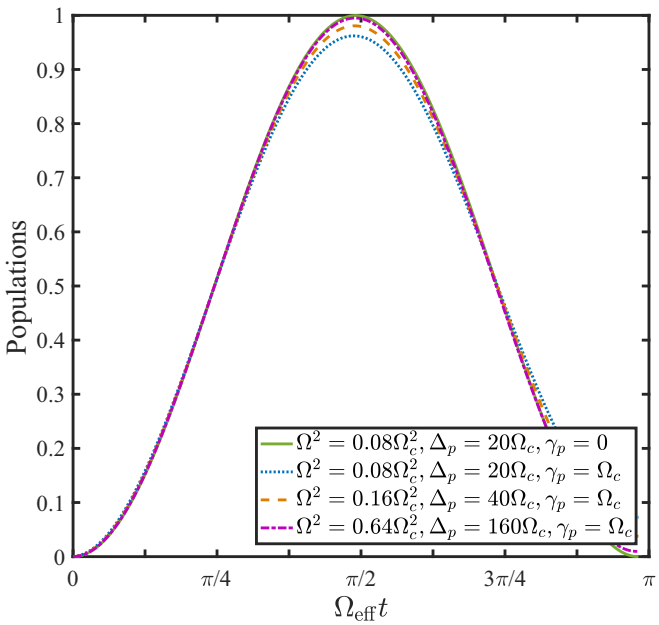

FIG. 3. Population of state $|e\rangle$ in the process of quantum state transfer for a single Λ-type atom versus a common dimensionless time $\Omega_{\rm eff}t$ with different detuning and decoherence parameters, where $\Omega = \Omega_a = \Omega_b$ is assumed for simplicity.

Δ_p does provide an immune way to the spontaneous emission of the atom.

The technology of a shortcut to adiabatic passage permits a fast manipulation of quantum states in a robust way against the fluctuation of parameters [34–38]. In order to design a counteradiabatic Hamiltonian that can be realized in experiment, we first consider a toy model below:

$$H_{\rm ap}(t) = \sqrt{2}\Omega_a^{'}(t)|gg\rangle\langle\Phi| + \Omega_b^{'}(t)|T\rangle\langle\Phi| + \text{H.c.}, \quad (10)$$

where $|\Phi\rangle = (|gp\rangle + |pg\rangle)/\sqrt{2}$. This Hamiltonian is equivalent to a simple three-level system with an excited state $|\Phi\rangle$ and two ground states $|gg\rangle$ and $|T\rangle$. The corresponding eigenstates can be easily obtained:

$$|n_0(t)\rangle = \cos[\theta(t)]|gg\rangle - \sin[\theta(t)]|T\rangle, \quad (11)$$

$$|n_\pm(t)\rangle = \frac{\sin[\theta(t)]}{\sqrt{2}}|gg\rangle \pm \frac{1}{\sqrt{2}}|\Phi\rangle + \frac{\cos[\theta(t)]}{\sqrt{2}}|T\rangle, \quad (12)$$

and the eigenvalues are $\varepsilon_0 = 0$ and $\varepsilon_\pm = \pm\Omega^{'}$, respectively, where $\theta(t) = \arctan[\sqrt{2}\Omega_a^{'}(t)/\Omega_b^{'}(t)]$ and $\Omega^{'} = \sqrt{2\Omega_a^{'2}(t) + \Omega_b^{'2}(t)}$. According to Berry's transitionless tracking algorithm [39], the simplest form of reverse engineering Hamiltonian $H_{\rm cap}(t)$, which is related to the original Hamiltonian $H_{\rm ap}(t)$, takes the form

$$H_{\rm cap}(t) = i\sum_{k=0,\pm}|\partial_t n_k(t)\rangle\langle n_k(t)|$$

$$= i\dot{\theta}(t)|gg\rangle\frac{1}{\sqrt{2}}(\langle ge| + \langle eg|) + \text{H.c.}, \quad (13)$$

where $\dot{\theta}(t) = \sqrt{2}[\dot{\Omega}_a^{'}(t)\Omega_b^{'}(t) - \Omega_a^{'}(t)\dot{\Omega}_b^{'}(t)]/\Omega^{'2}$. Comparing Eq. (13) with Eq. (5), we are able to obtain an alternative physically feasible Hamiltonian whose effect is equivalent to $H_{\rm cap}(t)$:

$$\widetilde{H}_{\rm eff} = i\frac{\Omega_{\rm cap}^2}{\Delta_p}|gg\rangle\frac{1}{\sqrt{2}}(\langle ge| + \langle eg|) + \text{H.c.}, \quad (14)$$

and the shortcut to adiabatic passage for preparation of bipartite entanglement can be achieved as long as $\Omega_a = i\Omega_{\rm cap}/\sqrt{2}$, $\Omega_b = \Omega_{\rm cap}$, and $\Omega_{\rm cap}^2/\Delta_p = \dot{\theta}(t)$, i.e.,

$$\Omega_{\rm cap}^2 = \Delta_{\rm p}\dot{\theta}(t) = \frac{\sqrt{2}\Delta_{\rm p}[\dot{\Omega}_a^{'}(t)\Omega_b^{'}(t) - \Omega_a^{'}(t)\dot{\Omega}_b^{'}(t)]}{\Omega^{'2}}, \quad (15)$$

where the Rabi frequencies $\Omega_a^{'}(t)$ and $\Omega_b^{'}(t)$ are chosen as

$$\Omega_a^{'}(t) = \Omega_0\exp\left[-\frac{(t - t_c/2 - \tau)^2}{T^2}\right], \quad (16)$$

$$\Omega_b^{'}(t) = \Omega_0\exp\left[-\frac{(t - t_c/2 + \tau)^2}{T^2}\right], \quad (17)$$

in order to satisfy the boundary condition of the stimulated Raman adiabatic passage on the one hand and meet the requirement of the following ground-state blockade effect for time-dependent Raman couplings on the other hand [40],

$$\left|\frac{1}{2}S(t_c)\right| = \left|\frac{i}{2}\int_0^{t_c} e^{-i\lambda(t_c - t)}\frac{\Omega_a(t)\Omega_b(t)}{\Delta_p}dt\right| \ll 1. \quad (18)$$

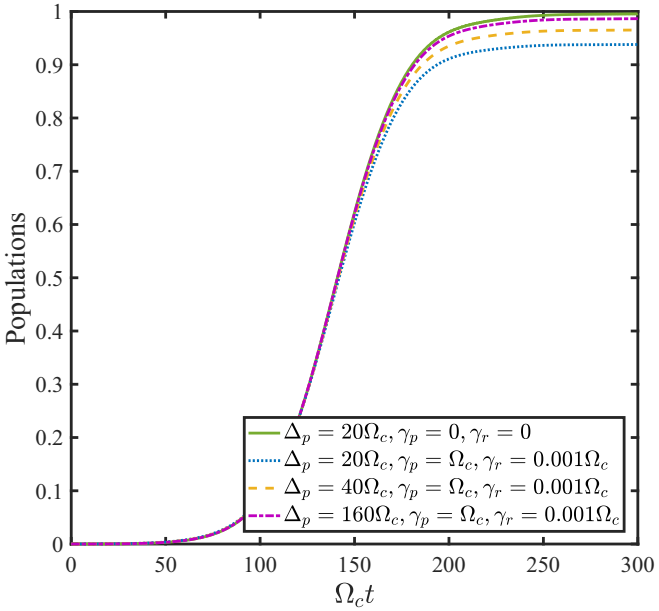

FIG. 4. Population of the maximally entangled state $(|ge\rangle + |eg\rangle)/\sqrt{2}$ during the shortcut to adiabatic passage versus dimensionless interaction time $\Omega_c t$ for different detuning and decoherence parameters. We have chosen $t_c = 300/\Omega_c$, $\tau = 0.2t_c$, and $T = 0.3t_c$ in Eqs. (16) and (17), and $\Delta_r = 20\Omega_c$.

We remark that Eq. (18) automatically degenerates to $|\Omega_{\rm eff}| \ll |\lambda|$ for the time-independent Raman couplings of Eq. (5) in the absence of Δ. In Fig. 4, we check the performance of the shortcut to adiabatic passage in the generation of the entangled state $(|ge\rangle + |eg\rangle)/\sqrt{2}$ from the initial state $|gg\rangle$ by setting the operation time $t_c = 300/\Omega_c$, $\tau = 0.2t_c$, and $T = 0.3t_c$. With the dissipation being considered, a conclusion the same as in the single-atom case can be made that a large detuning condition guarantees a high fidelity $F(t) = \text{Tr}\sqrt{\rho^{1/2}\rho(t)\rho^{1/2}} = \sqrt{P(t)} = 99.32\%$, corresponding to the dash-dotted line.

IV. STEADY ENTANGLEMENT VIA QUANTUM-JUMP-BASED FEEDBACK CONTROL

The above analysis has demonstrated that a regime of the ground-state blockade effect functioning well is also immune to the atomic decay. Therefore combined with cavity quantum electrodynamics, the ground-state blockade provides a novel approach to quantum state preparation, especially for the cavity-loss-induced generation of entangled atoms [41–43]. In this section, we consider an atom-cavity interaction system, as depicted in Fig. 5. The transition between the levels $|g\rangle \leftrightarrow |p\rangle$ is coupled to the cavity mode resonantly with coupling constant g. The transitions $|e\rangle \leftrightarrow |p\rangle$ and $|e\rangle \leftrightarrow |r\rangle$ are driven by nonresonant classical laser fields with Rabi frequencies Ω_b and Ω_c, respectively. The resonant coupling between ground states $|g\rangle$ and $|e\rangle$ is realized by a microwave field with Rabi frequency ω. Thus the master equation of system could be

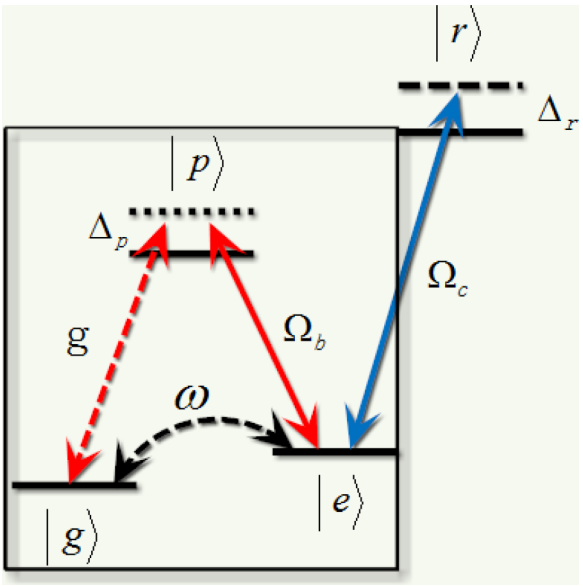

FIG. 5. Schematic view of the atomic-level configuration. Compared with Fig. 1, the transition $|g\rangle \leftrightarrow |p\rangle$ is replaced by a quantized cavity field mode with coupling strength g, and a resonant transition between $|g\rangle$ and $|e\rangle$ is driven by a microwave field with Rabi frequency ω.

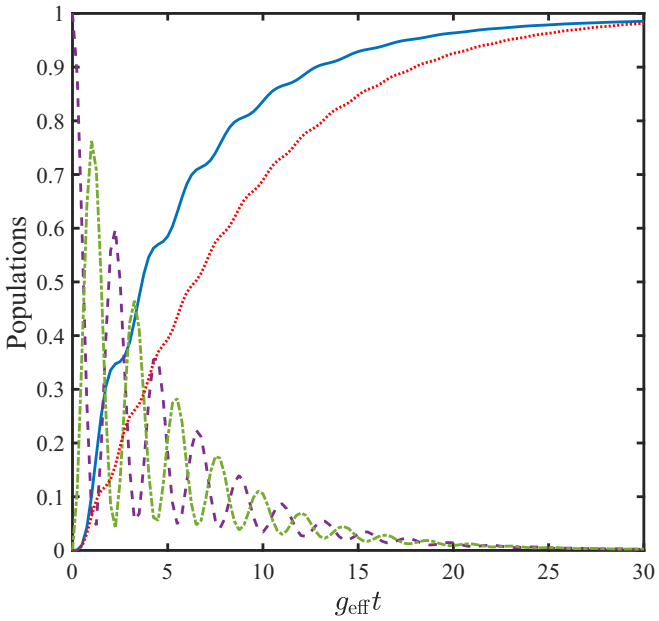

FIG. 6. Populations of quantum states versus dimensionless time $g_{\rm eff}t$ during preparation of the antisymmetric entangled state $|S\rangle$. Other parameters: $\omega = g_{\rm eff}$, $\kappa = \lambda = 10g_{\rm eff}$, and $\eta = -0.5\pi$.

written as

$$\dot{\rho} = -i[H_I^{'},\rho] + \frac{\gamma_p}{2}\sum_{n=1}^{2}(\mathcal{D}[|g\rangle_n\langle p|]\rho + \mathcal{D}[|e\rangle_n\langle p|]\rho) + \gamma_r\sum_{n=1}^{2}\mathcal{D}[|e\rangle_n\langle r|]\rho + \kappa\mathcal{D}[a]\rho, \tag{19}$$

where the Hamiltonian $H_I^{'} = \sum_{i=1}^{2} g|p\rangle_i\langle g|a + \Omega_b|p\rangle_i\langle e| + \Omega_c|r\rangle_i\langle e| + \omega|g\rangle_i\langle e| + \text{H.c.} - \Delta_p|p\rangle_i\langle p| + (U - 2\Delta_r)|rr\rangle\langle rr|$, γ_r is the decaying rate of the Rydberg state, a is the annihilation operator of the cavity mode, and κ is the loss rate of the cavity. After adiabatically eliminating the excited state $|p\rangle$ and the single-atom state $|r\rangle$, we have

$$H_{\rm eff}^{'} = \sum_{i=1}^{2}(g_{\rm eff}a^{\dagger} + \omega)|g\rangle_i\langle e| + \lambda|ee\rangle\langle rr| + \text{H.c.}, \tag{20}$$

where $g_{\rm eff} = g\Omega_b/\Delta_p$. In the regime of ground-state blockade, $\{g_{\rm eff},\omega\} \ll \lambda$, the double occupation of state $|ee\rangle$ is suppressed and the above Hamiltonian is further simplified to

$$H_{gb}^{'} = (g_{\rm eff}a^{\dagger} + \omega)|gg\rangle(\langle ge| + \langle eg|) + \text{H.c.}. \tag{21}$$

In this case, the effective master equation prompting the evolution of two atoms becomes

$$\dot{\rho}_r = -i[H_{gb}^{'},\rho_r] + \sum_{n=1}^{2}\mathcal{D}\left[R_{gp}^{'n}\right]\rho_r + \mathcal{D}\left[R_{ep}^{'n}\right]\rho_r + \kappa\mathcal{D}[a]\rho_r, \tag{22}$$

with

$$R_{gp}^{'} = \frac{\Omega_b}{\Delta_p}\sqrt{\frac{\gamma_p}{2}}|g\rangle\langle e|, \quad R_{ep}^{'} = \frac{\Omega_b}{\Delta_p}\sqrt{\frac{\gamma_p}{2}}|e\rangle\langle e| \tag{23}$$

being the effective decay operators from $|e\rangle$ to $|g\rangle$ and from $|e\rangle$ to $|e\rangle$, respectively. For a strongly damped cavity mode, $\kappa \gg \{g_{\rm eff},\omega\}$, we further adiabatically eliminate the populations of the cavity mode and acquire the master equation for the reduced density operator of atoms:

$$\dot{\rho}_r = -i\omega[(J_+ + J_-),\rho_r] + \Gamma\mathcal{D}[J_-]\rho_r, \tag{24}$$

where $J_- = J_+^{\dagger} = |gg\rangle(\langle eg| + \langle ge|)$ is the collective lowering operators of atoms and $\Gamma = 4g_{\rm eff}^2/\kappa$ is the collective amplitude damping rate. In Eq. (24), we also neglect the spontaneous emission terms by supposing $\Gamma \gg \gamma_p\Omega_b^2/(2\Delta_p^2)$. Once the local feedback scenario is introduced, the cavity output is measured by a photodetector whose signal provides the input to the application of the feedback operator $U_{\rm fb} = \exp[-i\eta(\sigma_x \otimes I)]$, and the unconditioned master equation for this case is derived as

$$\dot{\rho}_r = -i\omega[(J_+ + J_-),\rho_r] + \Gamma\mathcal{D}[U_{\rm fb}J_-]\rho_r. \tag{25}$$

Note the local feedback operator is approximated to $U_{\rm fb} = \exp[-i\eta(|g\rangle_1\langle e| + |e\rangle_1\langle g|) \otimes |g\rangle_2\langle g|]$, because of the ground-state blockade effect. A simple inspection shows $|S\rangle = (|ge\rangle - |eg\rangle)/\sqrt{2}$ is the unique stationary state solution of Eq. (25). In Fig. 6, we numerically simulate the populations of quantum states versus dimensionless time $g_{\rm eff}t$ during the preparation of the antisymmetric entangled state $|S\rangle$ from an initial state $|gg\rangle$ with parameters $\omega = g_{\rm eff}$, $\kappa = \lambda = 10g_{\rm eff}$, and $\eta = -0.5\pi$. It only takes $t = 13/g_{\rm eff}$ to make the population of state $|S\rangle$ exceed 90% for the current scheme (solid line), compared with $t = 18/g_{\rm eff}$ for the case where ground-state blockade is not considered (dotted line). In this sense, the effect of ground-state blockade can speed up the convergence time for state preparation in an open system.

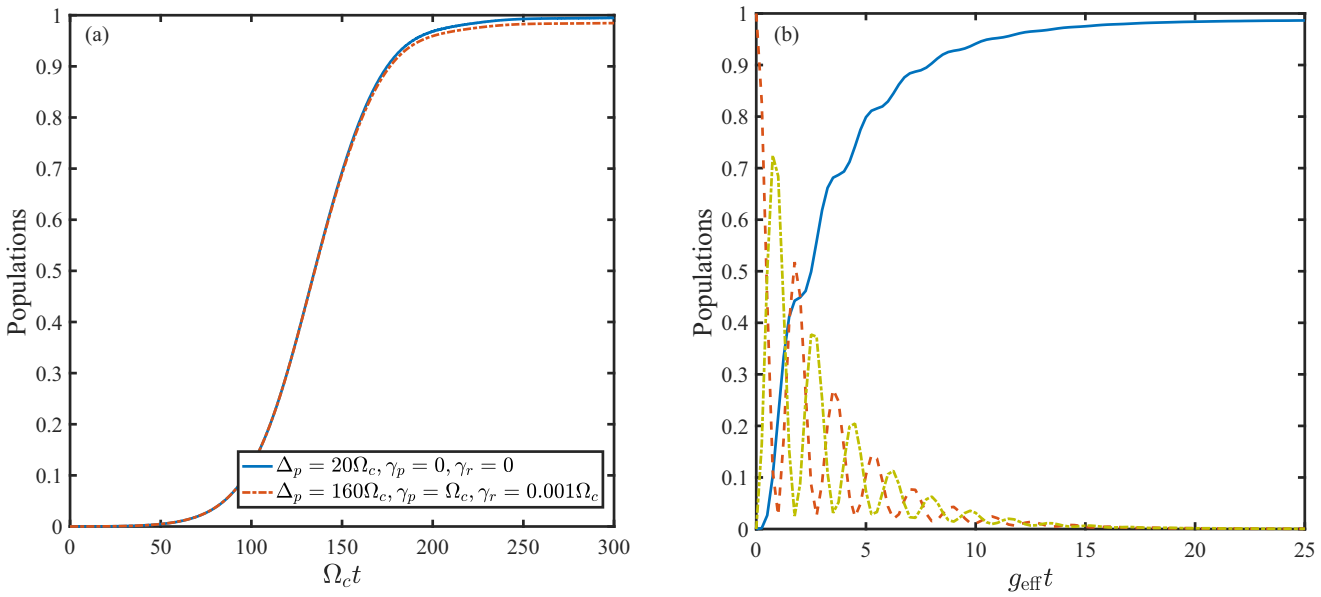

FIG. 7. (a) Population of W state during the shortcut to adiabatic passage versus dimensionless interaction time $\Omega_c t$. Other parameters are the same as those in Fig. 4. (b) Populations of quantum states versus dimensionless time $g_{\rm eff} t$ during preparation of the three-atom decoherence-free state $|\mathrm{DFS}\rangle$. Other parameters: $\omega = g_{\rm eff}$, $\kappa = 10 g_{\rm eff}$, $\lambda = 20 g_{\rm eff}$, and $\eta = -0.5\pi$.

V. GENERALIZATION TO THREE-ATOM ENTANGLEMENT

In the scheme of utilizing a shortcut to adiabatic passage, a three-atom W state $(|egg\rangle + |geg\rangle + |gge\rangle)/\sqrt{3}$ can be prepared straightforwardly with the following time-dependent Hamiltonian:

$$\widetilde{H}_{\rm eff} = \frac{\sqrt{3}\Omega_a(t)\Omega_b(t)}{\Delta_{\rm p}}|ggg\rangle\langle W| + \mathrm{H.c.}. \tag{26}$$

The counteradiabatic Hamiltonian is then received by selecting $\Omega_a = i\Omega_{\rm cap}/\sqrt{3}$, $\Omega_b = \Omega_{\rm cap}$, and

$$\Omega_{\rm cap}^2 = \Delta_{\rm p}\dot{\theta}(t) = \frac{\sqrt{3}\Delta_{\rm p}[\dot{\Omega}_a'(t)\Omega_b'(t) - \Omega_a'(t)\dot{\Omega}_b'(t)]}{\Omega'^2}, \tag{27}$$

where $\Omega' = \sqrt{3\Omega_a'^2(t) + \Omega_b'^2(t)}$. At the same time, the condition of ground-state blockade should be satisfied:

$$\left|\frac{i}{2}\int_0^{t_c} e^{-i\lambda(t_c - t)}\frac{\sqrt{2}\Omega_a(t)\Omega_b(t)}{\Delta_p}dt\right| \ll 1. \tag{28}$$

As for the quantum-feedback-based scheme, the local feedback operator on the first atom $U_{\rm fb} = \exp[-i\eta(|g\rangle_1\langle e| + |e\rangle_1\langle g|) \otimes |g_2\rangle\langle g_2| \otimes |g_3\rangle\langle g_3|]$, along with the dissipation of the cavity, will stabilize the system into a dark state of the collective lowering operator $J_- = |ggg\rangle(\langle egg| + \langle geg| + \langle gge|)$, i.e.,

$$|\mathrm{DFS}\rangle_N = \frac{1}{\sqrt{6}}(|gge\rangle + |geg\rangle - 2|egg\rangle). \tag{29}$$

Figure 7 shows the populations of three-atom entanglement as a function of time for both the closed system and the open system. In Fig. 7(a), the solid line indicates an ideal situation for the shortcut to adiabatic passage without dissipation, and the final fidelity of the entangled state is 99.74%. Even in the presence of spontaneous emission $\gamma_p = \Omega_c$ and $\gamma_r = 0.001\Omega_c$, a large detuning $\Delta_p = 160\Omega_c$ preserves the fidelity up to 99.23% (dash-dotted line). In Fig. 7(b), starting from the initial state $|ggg\rangle$, the population of the state $|ggg\rangle$ (dashed line) and the W state (dash-dotted line) undergo rapid coherent oscillation with an envelope decaying, while the three-atom decoherence-free state $|\mathrm{DFS}\rangle_3$ (solid line) converges to 99.32% at a short time $t = 25/g_{\rm eff}$ with parameters $\omega = g_{\rm eff}$, $\kappa = 10 g_{\rm eff}$, $\lambda = 20 g_{\rm eff}$, and $\eta = -0.5\pi$.

In experiment, the configuration of an N-type Rydberg atom can be found in the ^{87}Rb atom. The key components of our proposal are the Raman transition of two ground states and a two-photon transition between the ground state and the Rydberg state. In Ref. [44], the authors demonstrate a fast Rabi flopping at MHz between $5s_{1/2}$ ground hyperfine states $|0\rangle = |f = 1, m = 0\rangle$ and $|1\rangle = |f = 2, m = 0\rangle$ that are separated by 6.83 GHz of the neutral ^{87}Rb atom, where each ground state is coupled to the $5p_{3/2}$ excited by a detuning of $\Delta_p = 2\pi \times 41$ GHz. In Refs. [4,7], Browaeys *et al.* excite a ground state of $5s_{1/2}$ to the Rydberg state of $58d_{3/2}$ via a two-photon transition mediated by the optical state of $5p_{1/2}$, where an effective two-photon Rabi frequency $\Omega_c \approx 2\pi \times 7$ MHz is achieved. In Refs. [8,45], the entanglement of two neutral atoms and a corresponding controlled-NOT gate are also demonstrated with N-type Rydberg atoms. Referring to our model, the relevant energy level structure is shown in Fig. 8. The ground states $|g\rangle$ and $|e\rangle$ correspond to the atomic levels $|f = 1, m = 0\rangle$ and $|f = 2, m = 0\rangle$ of the $5s_{1/2}$ manifold; the excited state $|p\rangle$ corresponds to the $5p_{3/2}$ atomic state with a radiative decaying rate of $\gamma_p = 2\pi \times 3$ MHz, and the decaying rate of the $97d_{5/2}$ Rydberg state $\gamma_r \sim 2\pi \times 1$ kHz. The Raman transition between ground states $|g\rangle$ and $|e\rangle$ is accomplished by σ_+-polarized and π-polarized 780-nm laser beams both tuned to transit towards $|f = 2, m = 0\rangle$ of $5p_{3/2}$ by about $\Delta_p = 2\pi \times 3.2$ GHz. The

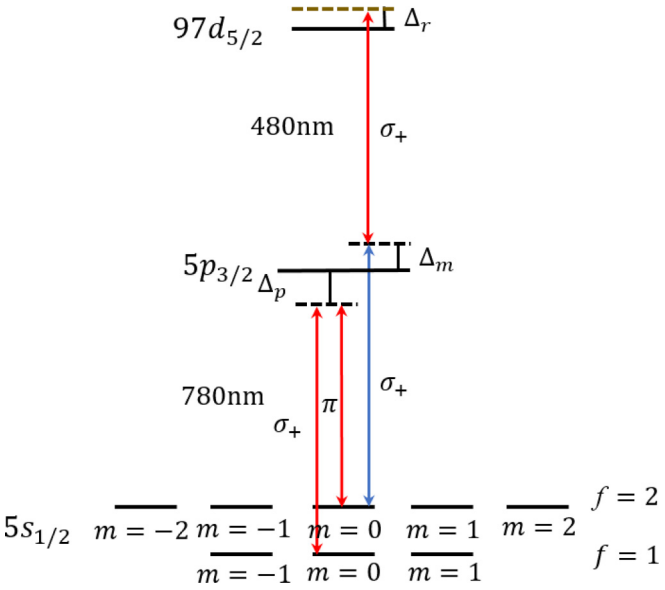

FIG. 8. Schematic view of the N-type Rydberg atom with the relevant energy level structure of the ^{87}Rb atom.

Rydberg excitation uses σ_+-polarized 780- and 480-nm beams tuned for excitation of the Rydberg state of $97d_{5/2}$, detuned by $\Delta_r = 2\pi \times 200$ MHz, leading to the coupling strength between $|e\rangle$ and $|r\rangle$ of order $\Omega_c \sim 2\pi \times 10$ MHz. Note that a two-photon transition between the ground state $|g\rangle$ and the excited Rydberg state $|r\rangle$ cannot happen due to a large detuning parameter, $\Delta_p + \Delta_m - \Delta_r$, on one hand, and the σ_+-polarized 480-nm laser beam is unable to couple $|f = 2, m = 0\rangle$ of $5p_{3/2}$ to other hyperfine levels of $97d_{5/2}$ based on the selection rule on the other hand. For the first scheme governed by the shortcut to adiabatic passage, the Rabi frequency $\Omega_{\rm cap}$ is completely determined by the value of the detuning parameter Δ_p, provided the operation time t_c is fixed. Hence we can obtain a high fidelity of two-atom entanglement of 99.14%. For the second scheme based on quantum feedback control, the experimentally available coupling strength between the atom and the cavity $g = 2\pi \times 14.4$ MHz and the cavity decaying rate $\kappa = 2\pi \times 0.66$ MHz should also be taken into account [46–48]. In this case, we choose $\Delta_p = 2\pi \times 1.44$ GHz and $\Omega_b = g$ in order to gain a fidelity of 98.95% at a short time of about $t = 50/g_{\rm eff} \approx 55.26\ \mu$s.

We remark that the theoretical assumption $\Delta = (U - 2\Delta_r + 2\Omega_c^2/\Delta_r) = 0$ made throughout this paper is only for the sake of convenient discussion. In fact, the Rydberg-mediated interaction U does not need to be limited to a specific value, as long as the approximation in Eq. (5) is effective. We take $\Delta = 5\Omega_{\rm eff}$ as an example, which can be extracted from Fig. 2. In this case, a selection of $\lambda = 20\Omega_{\rm eff}$ corresponding to $R_1 \approx 24.21$ and $R_2 \approx 16.65$ is able to block the maximal population of state $|ee\rangle$ at 5.18×10^{-4}. In this sense the mechanism of ground-state blockade proposed here can be implemented for a wide range of parameters.

VI. SUMMARY

In summary, we have investigated how to actualize a ground-state blockade effect via a weak Raman transition and a strong Rydberg antiblockade. This mechanism has prominent advantages in the preparation of the quantum entangled state, since it reserves the nonlinear Rydberg interaction and simultaneously provides a robust approach against the spontaneous emission of the atom. In our future study, we will concentrate on the application of the ground-state blockade in terms of quantum computing and quantum algorithm. We expect that our work may bring some new ideas on quantum information processing with neutral atoms.

ACKNOWLEDGMENTS

The authors thank the anonymous reviewer for constructive comments that helped to improve the quality of this paper. This work is supported by the Natural Science Foundation of China under Grants No. 11647308, No. 11674049, No. 11534002, and No. 61475033 and by Fundamental Research Funds for the Central Universities under Grant No. 2412016KJ004.

APPENDIX: DETAIL DERIVATION OF THE GROUND-STATE BLOCKADE HAMILTONIAN

In this appendix, we give the detail derivation of the ground-state blockade Hamiltonian of Eq. (5). According to Fig. 1, the Hamiltonian of our system in the Schrödinger picture reads ($\hbar = 1$)

$$H_S = H_0 + H_I, \tag{A1}$$

$$H_0 = \sum_{i=1}^{2} \omega_g |g\rangle_i\langle g| + \omega_e |e\rangle_i\langle e| + \omega_p |p\rangle_i\langle p| + \omega_r |r\rangle_i\langle r|,$$

$$H_I = \sum_{i=1}^{2} \Omega_a |p\rangle_i\langle g| e^{-i\omega_a t} + \Omega_b |p\rangle_i\langle e| e^{-i\omega_b t} + \Omega_c |r\rangle_i\langle e| e^{-i\omega_c t} + \text{H.c.} + U|rr\rangle\langle rr|,$$

where $\omega_j (j = g, e, p, r)$ describes the frequency of the atomic level $|j\rangle$ and $\omega_k (k = a, b, c)$ represents the driving frequency of the classical field corresponding to the Rabi frequency Ω_k. Thus in the interaction picture, we have

$$H_I = H_I^0 + H_I^1, \tag{A2}$$

$$H_I^0 = \sum_{i=1}^{2} \Omega_a |p\rangle_i\langle g| e^{-i\Delta_p t} + \Omega_b |p\rangle_i\langle e| e^{-i\Delta_p t} + \text{H.c.},$$

$$H_I^1 = \sqrt{2}\Omega_c |ee\rangle\langle\chi| e^{i\Delta_r t} + \sqrt{2}\Omega_c |rr\rangle\langle\chi| e^{i(\Delta_r + \delta)t} + \text{H.c.},$$

where we have introduced the state $|\chi\rangle = (|er\rangle + |re\rangle)/\sqrt{2}$ for simplicity and assumed the detuning parameters $\Delta_p = \omega_a - (\omega_p - \omega_g) = \omega_b - (\omega_p - \omega_e)$, $\Delta_r = \omega_c - (\omega_r - \omega_e)$, and $U = (2\Delta_r + \delta)$. Now the Hamiltonian H_I has been divided into two parts: one part, H_I^0, is the Raman interaction of atoms and the other part, H_I^1, is the two-photon transition. In the regime of the large detuning limit $\Delta_p \gg \{\Omega_a, \Omega_b\}$, we can adiabatically eliminate the excited state $|p\rangle$ and obtain the effective form of H_I^0 with the Stark-shift term of the state

$|g\rangle(|e\rangle)$ and the effective Rabi frequency:

$$\frac{\langle g(e)|H_I^0|p\rangle\langle p|H_I^0|g(e)\rangle}{\Delta_p} = \frac{\Omega_{a(b)}^2}{\Delta_p}, \tag{A3}$$

$$\frac{\langle g(e)|H_I^0|p\rangle\langle p|H_I^0|e(g)\rangle}{\Delta_p} = \frac{\Omega_a\Omega_b}{\Delta_p}. \tag{A4}$$

Similarly, the large detuning condition $\Delta_r \gg \Omega_c$ permits us to eliminate the mediate state $|\chi\rangle$; then H_I^1 reduces to an equivalent form with two-atom Stark shifts of levels $|ee\rangle$ and $|rr\rangle$ and effective coupling between them:

$$\frac{\langle ee|H_I^1|\chi\rangle\langle\chi|H_I^1|ee\rangle}{\Delta_r} = \frac{2\Omega_c^2}{\Delta_r}, \tag{A5}$$

$$\frac{\langle rr|H_I^1|\chi\rangle\langle\chi|H_I^1|rr\rangle}{\Delta_r+\delta} \approx \frac{2\Omega_c^2}{\Delta_r}, \tag{A6}$$

$$\frac{\langle rr|H_I^1|\chi\rangle\langle\chi|H_I^1|ee\rangle}{\overline{\Delta}_r} \approx \frac{2\Omega_c^2}{\Delta_r}e^{i\delta t}, \tag{A7}$$

$$\frac{\langle ee|H_I^1|\chi\rangle\langle\chi|H_I^1|rr\rangle}{\overline{\Delta}_r} \approx \frac{2\Omega_c^2}{\Delta_r}e^{-i\delta t}, \tag{A8}$$

where $\delta \ll \Delta_r$ has been assumed and $1/\overline{\Delta}_r = [1/\Delta_r + 1/(\Delta_r+\delta)]/2 \approx 1/\Delta_r$ [49], i.e.,

$$\begin{aligned} H_{\text{eff}} = &\sum_{i=1}^{2}\frac{\Omega_a^2}{\Delta_p}|g\rangle_i\langle g| + \left(\frac{\Omega_b^2}{\Delta_p}+\frac{\Omega_c^2}{\Delta_r}\right)|e\rangle_i\langle e| \\ &+\left[\frac{2\Omega_c^2}{\Delta_r}|ee\rangle\langle rr|e^{-i\delta t} + \sum_{i=1}^{2}\frac{\Omega_a\Omega_b}{\Delta_p}|g\rangle_i\langle e| + \text{H.c.}\right] \\ &+\frac{2\Omega_c^2}{\Delta_r}|rr\rangle\langle rr|. \end{aligned} \tag{A9}$$

The Stark shifts of ground states are unwanted in our proposal, which can be canceled by other ancillary levels yielding opposite shifts of energy levels. After performing a rotation with respect to $U = \exp(i\delta t|rr\rangle\langle rr|)$, Eq. (A9) is rewritten in the following time-independent form:

$$H_{\text{eff}} = \sum_{i=1}^{2}\Omega_{\text{eff}}|g\rangle_i\langle e| + \lambda|ee\rangle\langle rr| + \text{H.c.} + \Delta|rr\rangle\langle rr|, \tag{A10}$$

where $\Omega_{\text{eff}} = \Omega_a\Omega_b/\Delta_p$, $\lambda = 2\Omega_c^2/\Delta_r$, and $\Delta = \delta + 2\Omega_c^2/\Delta_r$. In order to further characterize the effective dynamics of the system, we introduce the eigenstates of the two-atom transition Hamiltonian $(\lambda|ee\rangle\langle rr| + \text{H.c.} + \Delta|rr\rangle\langle rr|)$ as follows:

$$|\Psi_+\rangle = \cos\alpha|rr\rangle + \sin\alpha|ee\rangle \tag{A11}$$

and

$$|\Psi_-\rangle = \sin\alpha|rr\rangle - \cos\alpha|ee\rangle, \tag{A12}$$

which correspond to eigenvalues $E_+ = (\Delta + \sqrt{\Delta^2+4\lambda^2})/2$ and $E_- = (\Delta - \sqrt{\Delta^2+4\lambda^2})/2$, respectively, with $\alpha = \arctan[2\lambda/(\Delta+\sqrt{\Delta^2+4\lambda^2})]$. Through the above steps, we recover the result of Eq. (4). The derivation from Eq. (4) to Eq. (5) is straightforward as long as the limiting conditions $R_1 = |E_+/(\sqrt{2}\Omega_{\text{eff}}\sin\alpha)| \gg 1$ and $R_2 = |E_-/(\sqrt{2}\Omega_{\text{eff}}\cos\alpha)| \gg 1$ are established. To better illustrate this process, we perform another rotation with respect to $\exp[-it(E_+|\Psi_+\rangle\langle\Psi_+| + E_-|\Psi_-\rangle\langle\Psi_-|)]$ on the basis of Eq. (4) and obtain

$$\begin{aligned} H_{\text{eff}} = &\sqrt{2}\Omega_{\text{eff}}|gg\rangle\langle T| + (\sqrt{2}\Omega_{\text{eff}}\sin\alpha e^{iE_+t}|\Psi_+\rangle \\ &-\sqrt{2}\Omega_{\text{eff}}\cos\alpha e^{iE_-t}|\Psi_-\rangle)\langle T| + \text{H.c.}, \end{aligned} \tag{A13}$$

where $|T\rangle = (|ge\rangle + |eg\rangle)/\sqrt{2}$. It can be seen clearly that the Hamiltonian of Eq. (A13) incorporates the high-frequency oscillating terms proportional to $\exp(iE_\pm t)$, and these terms can be neglected while the resonant transition between states $|gg\rangle$ and $|T\rangle$ is preserved; hence a perfect ground-state blockade Hamiltonian of Eq. (5) is achieved.

[1] D. Jaksch, J. I. Cirac, P. Zoller, S. L. Rolston, R. Côté, and M. D. Lukin, Phys. Rev. Lett. **85**, 2208 (2000).

[2] M. D. Lukin, M. Fleischhauer, R. Cote, L. M. Duan, D. Jaksch, J. I. Cirac, and P. Zoller, Phys. Rev. Lett. **87**, 037901 (2001).

[3] E. Urban, T. A. Johnson, T. Henage, L. Isenhower, D. D. Yavuz, T. G. Walker, and M. Saffman, Nat. Phys. **5**, 110 (2009).

[4] A. Gaëtan, Y. Miroshnychenko, T. Wilk, A. Chotia, M. Viteau, D. Comparat, P. Pillet, A. Browaeys, and P. Grangier, Nat. Phys. **5**, 115 (2009).

[5] D. Møller, L. B. Madsen, and K. Mølmer, Phys. Rev. Lett. **100**, 170504 (2008).

[6] M. Saffman and K. Mølmer, Phys. Rev. Lett. **102**, 240502 (2009).

[7] T. Wilk, A. Gaëtan, C. Evellin, J. Wolters, Y. Miroshnychenko, P. Grangier, and A. Browaeys, Phys. Rev. Lett. **104**, 010502 (2010).

[8] X. L. Zhang, L. Isenhower, A. T. Gill, T. G. Walker, and M. Saffman, Phys. Rev. A **82**, 030306 (2010).

[9] A. Chen, Opt. Express **19**, 2037 (2011).

[10] K. Mølmer, L. Isenhower, and M. Saffman, J. Phys. B **44**, 184016 (2011).

[11] D. D. Bhaktavatsala Rao and K. Mølmer, Phys. Rev. A **86**, 042321 (2012).

[12] H. Weimer, M. Müller, I. Lesanovsky, P. Zoller, and H. P. Büchler, Nat. Phys. **6**, 382 (2010).

[13] A. Dauphin, M. Müller, and M. A. Martin-Delgado, Phys. Rev. A **86**, 053618 (2012).

[14] S. Baur, D. Tiarks, G. Rempe, and S. Dürr, Phys. Rev. Lett. **112**, 073901 (2014).

[15] E. Brion, L. H. Pedersen, M. Saffman, and K. Mølmer, Phys. Rev. Lett. **100**, 110506 (2008).

[16] Y. Han, B. He, K. Heshami, C.-Z. Li, and C. Simon, Phys. Rev. A **81**, 052311 (2010).

[17] B. Zhao, M. Müller, K. Hammerer, and P. Zoller, Phys. Rev. A **81**, 052329 (2010).
[18] C. Ates, T. Pohl, T. Pattard, and J. M. Rost, Phys. Rev. Lett. **98**, 023002 (2007).
[19] T. Amthor, C. Giese, C. S. Hofmann, and M. Weidemüller, Phys. Rev. Lett. **104**, 013001 (2010).
[20] A. W. Carr and M. Saffman, Phys. Rev. Lett. **111**, 033607 (2013).
[21] X.-Q. Shao, T.-Y. Zheng, C. H. Oh, and S. Zhang, Phys. Rev. A **89**, 012319 (2014).
[22] X.-Q. Shao, T.-Y. Zheng, C. H. Oh, and S. Zhang, J. Opt. Soc. Am. B **31**, 827 (2014).
[23] S.-L. Su, Y. Gao, E. Liang, and S. Zhang, Phys. Rev. A **95**, 022319 (2017).
[24] M. Saffman, J. Phys. B **49**, 202001 (2016).
[25] M. Saffman, T. G. Walker, and K. Mølmer, Rev. Mod. Phys. **82**, 2313 (2010).
[26] P. Facchi, H. Nakazato, and S. Pascazio, Phys. Rev. Lett. **86**, 2699 (2001).
[27] P. Facchi, V. Gorini, G. Marmo, S. Pascazio, and E. Sudarshan, Phys. Lett. A **275**, 12 (2000).
[28] P. Facchi and S. Pascazio, J. Phys. A: Math. Theor. **41**, 493001 (2008).
[29] D. Comparat and P. Pillet, J. Opt. Soc. Am. B **27**, A208 (2010).
[30] L. Béguin, A. Vernier, R. Chicireanu, T. Lahaye, and A. Browaeys, Phys. Rev. Lett. **110**, 263201 (2013).
[31] J. Metz and A. Beige, Phys. Rev. A **76**, 022331 (2007).
[32] R. Stevenson, A. Carvalho, and J. Hope, Eur. Phys. J. D **61**, 523 (2011).
[33] X. Q. Shao, Z. H. Wang, H. D. Liu, and X. X. Yi, Phys. Rev. A **94**, 032307 (2016).
[34] X. Chen, I. Lizuain, A. Ruschhaupt, D. Guéry-Odelin, and J. G. Muga, Phys. Rev. Lett. **105**, 123003 (2010).
[35] Y.-H. Chen, Y. Xia, Q.-Q. Chen, and J. Song, Phys. Rev. A **89**, 033856 (2014).
[36] M. Lu, Y. Xia, L.-T. Shen, J. Song, and N. B. An, Phys. Rev. A **89**, 012326 (2014).
[37] Y.-X. Du, Z.-T. Liang, Y.-C. Li, X.-X. Yue, Q.-X. Lv, W. Huang, X. Chen, H. Yan, and S.-L. Zhu, Nat. Commun. **7**, 12479 (2016).
[38] Y.-H. Chen, Y. Xia, Q.-C. Wu, B.-H. Huang, and J. Song, Phys. Rev. A **93**, 052109 (2016).
[39] M. Berry, J. Phys. A: Math. Theor. **42**, 365303 (2009).
[40] Y. Li, C. Bruder, and C. P. Sun, Phys. Rev. A **75**, 032302 (2007).
[41] A. R. R. Carvalho and J. J. Hope, Phys. Rev. A **76**, 010301(R) (2007).
[42] A. R. R. Carvalho, A. J. S. Reid, and J. J. Hope, Phys. Rev. A **78**, 012334 (2008).
[43] R. N. Stevenson, J. J. Hope, and A. R. R. Carvalho, Phys. Rev. A **84**, 022332 (2011).
[44] D. D. Yavuz, P. B. Kulatunga, E. Urban, T. A. Johnson, N. Proite, T. Henage, T. G. Walker, and M. Saffman, Phys. Rev. Lett. **96**, 063001 (2006).
[45] L. Isenhower, E. Urban, X. L. Zhang, A. T. Gill, T. Henage, T. A. Johnson, T. G. Walker, and M. Saffman, Phys. Rev. Lett. **104**, 010503 (2010).
[46] F. Brennecke, T. Donner, S. Ritter, T. Bourdel, M. Köhl, and T. Esslinger, Nature (London) **450**, 268 (2007).
[47] C. Guerlin, E. Brion, T. Esslinger, and K. Mølmer, Phys. Rev. A **82**, 053832 (2010).
[48] X.-F. Zhang, Q. Sun, Y.-C. Wen, W.-M. Liu, S. Eggert, and A.-C. Ji, Phys. Rev. Lett. **110**, 090402 (2013).
[49] D. James and J. Jerke, Can. J. Phys. **85**, 625 (2007).